Remote Sensing of Environment 114 (2010) 2431–2435

Contents lists available at ScienceDirect

Remote Sensing of Environment

journal homepage: www.elsevier.com/locate/rse

Assessing canopy mortality during a mountain pine beetle outbreak using GeoEye-1 high spatial resolution satellite data

Philip E. Dennison *, Andrea R. Brunelle, Vachel A. Carter

Department of Geography, University of Utah, 260 S Central Campus Dr., Room 270, Salt Lake City, UT 84112, USA

ARTICLE INFO

Article history:
Received 13 December 2009
Received in revised form 16 May 2010
Accepted 16 May 2010

Keywords:
Mountain pine beetle
Lodgepole pine
Red attack
Gray attack
GeoEye-1

ABSTRACT

Continuing, severe outbreaks of mountain pine beetle (*Dendroctonus ponderosae*) across western North America have resulted in widespread mortality of lodgepole pine (*Pinus contorta*). Multiple studies have used high spatial resolution satellite data to map areas of beetle kill; these studies have largely focused on mapping red canopy cover associated with recent tree mortality and have not examined mapping gray canopy cover that occurs after red needles have dropped. The work presented here examines the use of newly available GeoEye-1 data for mapping both red and gray canopy area in southeastern Wyoming lodgepole pine forest. A 0.5 m spatial resolution, pan-sharpened GeoEye-1 image was used to classify areas of green, red, and gray canopy cover. Reference data were collected at twelve 500 m^2 field plots. Shadow-normalized green, red, and gray canopy area from classified GeoEye-1 data closely agreed with field-estimated green, red, and gray canopy area. Mean absolute error in canopy cover for the twelve sample plots was 8.3% for the green class, 5.4% for the red class, and 7.2% for the gray class. When all twelve plots were aggregated, remotely sensed estimates of green, red, and gray cover were within 1.7% of the field-estimated cover. Our results demonstrate that high spatial resolution spaceborne multispectral data are a promising tool for mapping canopy mortality caused by mountain pine beetle outbreaks.

1. Introduction

Bark beetles within the genus *Dendroctonus* are important drivers of ecological change in many forest ecosystems in western North America (Schmid & Hinds, 1974; Veblen et al., 1994; Schmid & Mata, 1996; Dale et al., 2001). Outbreaks of multiple bark beetle species are currently occurring simultaneously across the western United States and Canada. Drought stress, land management practices, and climate change have been implicated in recent outbreaks (e.g. Logan & Bentz, 1999; Breshears et al., 2005). One species of bark beetle, the mountain pine beetle (*D. ponderosae* Hopkins), has been infesting lodgepole pine forests at historically unprecedented rates. These massive outbreaks have important consequences that include lost timber, damaged recreational value, and altered ecosystem function (Amman & Schmitz, 1988; Logan & Powell, 2001).

The mountain pine beetle life cycle begins in late summer, when adult beetles stage coordinated attacks on live trees. Healthy trees may be able to fend off the attacking beetles by producing pitch, but stressed or diseased trees are more susceptible to successful attack. When adult beetles burrow into the bark to mate and lay eggs, they also inoculate the attacked tree with a tissue-damaging blue stain fungus (*Ophiostoma* spp.). The larvae develop galleries in the phloem over the next one to three seasons, and along with the action of the fungus, disrupt water and nutrient transport (Amman & Cole, 1983; Safranyik & Carroll, 2006). Foliage remains green as the tree is killed. In the year following the beetle attack, the tree canopy changes color as green chlorophyll, yellow carotene, and red anthocyanin pigments are successively degraded (Hill et al., 1967; Wulder et al., 2006a). The canopy first fades from green to yellow, followed by the canopy turning red, a stage called "red attack". Over a period lasting several months, the dead trees shed their red needles. The resulting needleless, gray canopy is referred to as the "gray attack" stage.

Multiple recent studies have used high spatial resolution satellite data to measure the impacts of mountain pine beetle infestations on western North American forests. White et al. (2005) used Ikonos 4 m resolution multispectral data to detect red attack in areas with low-to-moderate beetle infestations. Coops et al. (2006) found that a ratio of red reflectance to green reflectance, named the Red-Green Index (RGI), was superior for separating green, non-attacked tree crowns from red tree crowns using 2.5 m resolution multispectral Quickbird data. White et al. (2007) used Quickbird data to calculate RGI for detection of red crowns, and the resulting map of red canopy cover was used as reference data for coarser spatial resolution moisture indices calculated from Hyperion hyperspectral data. Wulder et al. (2008) examined a change detection approach to mapping red canopy area. Multiple dates of Quickbird data were used to calculate a ΔRGI, which was then used to map beetle attack progression in clusters of tree canopies. Also using Quickbird data, Hicke and Logan (2009) applied a

* Corresponding author. Tel.: +1 801 585 1805.
E-mail address: dennison@geog.utah.edu (P.E. Dennison).

0034-4257/$ – see front matter © 2010 Elsevier Inc. All rights reserved.
doi:10.1016/j.rse.2010.05.018

maximum likelihood classifier to separate 4 classes of land cover: green herbaceous, brown herbaceous, green canopy, and red canopy. Hicke and Logan (2009) accounted for illumination variability in complex terrain by stratifying spectral indices by solar incidence angle.

Previous studies using high resolution satellite data to map mountain pine beetle impacts have focused almost exclusively on the red attack stage of tree mortality. These studies have not assessed the ability of high spatial resolution satellite data to map gray canopy cover, the final stage of tree mortality (Wulder et al., 2006a). While gray canopy cover does not necessarily indicate mortality caused by mountain pine beetle, multitemporal remote sensing data (e.g. Wulder et al., 2008) could be used to monitor the progression of an outbreak by mapping both red and gray canopy cover over time. Previous work using satellite remote sensing has also been limited to the spatial resolution of data provided by the Ikonos and Quickbird sensors (White et al., 2005; Coops et al., 2006; Wulder et al., 2008; Hicke & Logan, 2009). GeoEye-1 is the first of a new generation of higher spatial resolution commercial satellite sensors, and its higher resolution may offer improved detection of mountain pine beetle impacts. The objective of this study was to examine the ability of 0.5 m spatial resolution, pan-sharpened GeoEye-1 data to accurately map percentages of green, red, and gray forest canopy cover in a mountain pine beetle-infested lodgepole pine forest in southeastern Wyoming.

2. Methods

Green, red and gray canopy cover were assessed using field measurements and remotely sensed data for the watershed of Long Lake, Wyoming, USA. Long Lake (40° 30′ N, 106° 22′ W) is located in the Snowy Mountain range, within Medicine Bow National Forest in southeastern Wyoming. The lake's watershed is small, with a forested land surface area of approximately 22 ha. The entire watershed was logged during the early 1900s. The forest in the watershed is dominated by two tree species: lodgepole pine (*Pinus contorta*) and subalpine fir (*Abies lasiocarpa*). A third tree taxon, Engelmann spruce (*Picea engelmannii*), is also found infrequently within the watershed. A recent mountain pine beetle outbreak has heavily impacted lodgepole pine within the forest surrounding Long Lake, killing many of the mature trees and resulting in large numbers of red and gray tree canopies.

Tree condition was measured within twelve 500 m^2 plots in September and October, 2009. For 10 of the plots, a GPS was used to find plot center coordinates that were randomly located within the Long Lake watershed. For the remaining 2 plots, the plot centers were located in stands high percentages of red (plot 3) or gray (plot 2) canopy cover. For all 12 plots, the coordinates of a stake placed in the center of the plot were measured using differential GPS. Circular plots were then created by measuring a radius of 12.62 m from the stake. Diameter at breast height (DBH) was measured for all trees with trunks within each plot. The distance and bearing to all trees with a DBH ≥ 5 cm was then measured using a laser rangefinder. For each tree with a DBH ≥ 5 cm, a condition code was also assigned (Wulder et al., 2006b). The condition code was based on visually-assessed canopy color, the percentage of needles retained by the tree, and on the presence of beetle boreholes in the tree bole. The condition code descriptions are summarized in Table 1. Although lodgepole pine is the only species at this site that is attacked by mountain pine beetles, the code values were also recorded for subalpine fir and Engelmann spruce. Dead trees of all species were assigned code 5, although mortality of some of the lodgepole pine and all of the fir and spruce was likely not caused by mountain pine beetle infestation. Condition codes were aggregated to match classes generated from image classification. Codes 0, 1, and 2 were grouped to form a green canopy class. Note that this class can contain both attacked and non-attacked lodgepole pine, as well as subalpine fir and Englemann spruce with green canopies.

Table 1
Condition codes used for assessing tree characteristics within each 500 m^2 plot. Boreholes are the entry holes of bark beetles, and the presence of these holes and pitch emitted from the holes was used as evidence of beetle attack for trees with green needles. N/A (not applicable) indicates that boreholes or pitch tubes were not used as a criterion for assigning codes 2–5.

Code	Tree status	Canopy appearance	Boreholes/pitch tubes
0	Live and not infested	Needles green	Absent
1	Current beetle attack	Needles green	Present
2	"Fader"	Needles light green or yellow	N/A
3	Red attack	Needles orange or red, canopy appears full and most or all needles retained	N/A
4	"Old" red attack	Needles orange or red, some needles appear to be missing but at least 30% of needles retained	N/A
5	Gray	0–30% of needles retained	N/A

Codes 3 and 4 were grouped to form a red canopy class. Finally, code 5 was assigned to a gray canopy class.

To obtain an estimate of canopy area within each of these color classes, an allometric equation relating DBH to canopy diameter was created. Canopy diameter was measured in two orthogonal directions for 5–10 trees within each plot. A total of 88 lodgepole pine, 48 subalpine fir, and 5 Engelmann spruce trees were measured. The two canopy diameter measurements were averaged, and regressed against DBH (Fig. 1). Regression parameters and the R^2 value for the pooled data (all three species) were similar to those for lodgepole pine and subalpine fir alone. Regression parameters for green and gray lodgepole pines alone were also similar to the parameters for the pooled regression. Regressing canopy diameter against DBH for lodgepole pines with red canopies produced a steeper slope and a negative intercept, likely due to underrepresentation of smaller diameter trees attacked by mountain pine beetle. The regression equation for the pooled data was believed to be more robust than equations for individual species and canopy color classes, and was used for further analysis:

$$canopy\,diameter\,(\mathrm{cm}) = 7.9778 \times DBH\,(\mathrm{cm}) + 71.264. \quad (1)$$

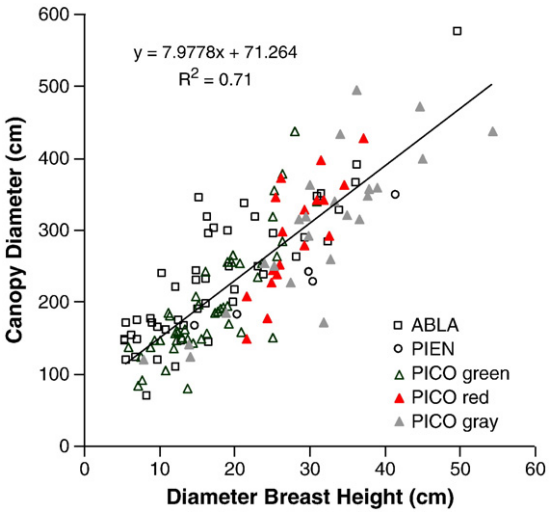

Fig. 1. Allometric relationship between diameter breast height and canopy diameter for all measured trees in the 12 sample plots. ABLA is subalpine fir (*Abies lasiocarpa*), PICO is lodgepole pine (*Pinus contorta*), and PIEN is Engelmann spruce (*Picea engelmannii*).

Eq. (1) was applied to all DBH values within each plot, and the resulting canopy diameter was used to calculate canopy area within the plot for the green, red, and gray cover classes. Canopies were assumed to have a circular footprint and to be non-overlapping.

A GeoEye-1 image was acquired for the watershed on 28 August 2009. GeoEye-1 has four spectral bands, with spectral ranges of 450–510 nm (blue), 510–580 nm (green), 655–690 nm (red), and 780–920 nm (near infrared). These four bands have an approximate spatial resolution of 1.65 m (GeoEye, 2009). GeoEye-1 also has a higher resolution panchromatic band that covers a spectral range from 450 to 800 nm. The GeoEye-1 image was acquired at 12:12 Mountain Daylight Time (18:12 UTC). At the time of acquisition, the local solar zenith angle was 34.2° and the local solar azimuth angle was 155.7°. The view zenith angle and view azimuth angles for the image were 17.0° and 291.2°, respectively. The 135.5° difference in solar and view azimuth angles created extensive shadowing in areas with forest cover. In addition, the 17° view zenith angle resulted in treetop displacement of up to 6 m and distorted canopy shape.

The standard pan-sharpened GeoEye-1 product, which fuses the multispectral and panchromatic bands to create a 0.5 m spatial resolution multispectral image, was used for mapping green, red, and gray forest cover. The proprietary fusion algorithm used by GeoEye does not preserve absolute radiance, so the Long Lake image was not corrected to apparent surface reflectance. Instead, the raw brightness values from the pan-sharpened image were used for classification. The GeoEye-1 product was terrain rectified by the image provider, but spatial registration was further improved to an absolute accuracy of approximately 2 m using a first-degree polynomial warp to 18 ground control points collected in the field using differential GPS.

Fig. 2 shows a portion of the GeoEye-1 image. Although mean canopy diameter within the plots was 2.4 m, trees were sometimes closely spaced and individual canopies were not distinguishable for smaller diameter trees. Visual interpretation was used to select 200 training pixels within each of 4 spectral classes: green canopy, red canopy, gray canopy, and shadow. The training pixels were selected from areas not covered by the sample plots, and from multiple locations within the watershed. A maximum likelihood classifier (ENVI, ITT Visual Information Systems) was trained using the training data and applied to the entire image. Both forested and non-forested areas of the image were classified by the green, red, gray, and shadow classes (Fig. 2). Non-forest cover was manually masked after classification to calculate green, red, and gray canopy cover over the entire study area.

Pixels within each sample plot were extracted from the classified image. The percent cover of the green, red, gray, and shadow classes was then calculated for each plot. For comparison with sample plot data, the class percentages were "shadow-normalized": the percent cover of each class was divided by the sum of all non-shadow class percentages. The shadow-normalized class percentages were then compared to field-sampled percent canopy cover using linear regression.

3. Results

A total of 957 trees were measured within the 12 sample plots (Table 2). Approximately two-thirds of the trees were lodgepole pine, with a mean DBH of 18.9 cm. Most of the remaining trees were subalpine fir, with a mean DBH of 12.9 cm. A total of 10 Engelmann spruce were measured. These trees had a mean DBH of 21.7 cm. Lodgepole pine was the dominant tree species in all but two of the plots. Lodgepole pine percent cover based on the area of the 500 m^2 plots ranged from 25.3% to 65.8%, with a mean of 44.3%. Expressed as a percentage of canopy area instead of plot area, lodgepole pine was subdominant at plots 1 (43.3%) and 12 (42.3%). In all other plots, lodgepole pine accounted for at least 65% of total canopy cover.

Subalpine fir were almost exclusively assigned condition codes 0 or 5. All condition codes were represented in lodgepole pine, with 0 being most prevalent code, followed by 5. Unattacked lodgepole pine (code 0) had a much lower mean DBH of 13.9 cm compared to the 24.0 cm mean DBH of attacked lodgepole pine (codes 1–5). Several Engelmann spruce did have boreholes in their trunks, but these were caused by a spruce bark beetle (*Dendroctonus rufipennis*), rather than mountain pine beetle.

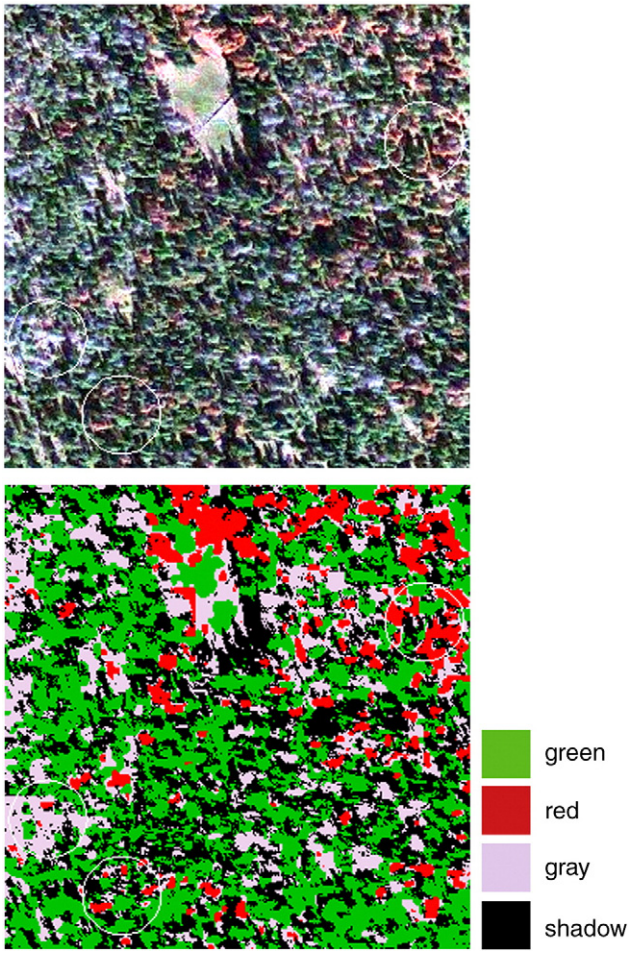

Fig. 2. The top image is a 150 m by 150 m subset, true-color composite of the pan-sharpened GeoEye-1 data. The bottom image is the maximum likelihood classification of the same area shown in the top image. The locations of three 12.62 m radius plots (circles) are shown in each image. Plot 2 is adjacent to the left edge of the image, plot 12 is adjacent to the bottom edge of the image, and plot 3 is adjacent to the right edge of the image.

Cover resulting from canopy diameter calculated using Eq. (1) indicated that an average of 40%, and up to 67%, of each plot was not covered by the canopy overstory. Herbaceous vegetation and low shrubs were present at all sites, but no spatial information on the cover of understory vegetation was collected. However, most of the

Table 2
Number of trees measured for all sample plots, by condition code and species.

Code	Species			Total
	ABLA	PICO	PIEN	
0	283	318	5	606
1	0	49	4	53
2	1	13	0	14
3	0	61	0	61
4	0	34	0	34
5	39	149	1	189
Total	323	624	10	957

canopy gap areas in each plot were heavily shadowed or covered by displaced treetops in the GeoEye-1 image. As a result, the comparison between field-measured and classified image data used the cover of green, red, and gray classes expressed as a percentage of canopy area, rather than plot area.

All 0.5 m pixels in the GeoEye-1 image were classified as green, red, gray, or shadow. These 4 classes appear to be appropriately assigned in forested areas (Fig. 2). Non-forested areas, such as clearings, roads, and water, were not included in the training data and thus were mapped as one of the four trained classes. For example, a clearing shown at top center in Fig. 2 was mapped as green, red, or gray depending on the spectral signature of the vegetation and litter covering the ground within the clearing.

Approximately 2000 0.5 m pixels fell within each sample plot area. The shadow class comprised between 22.5% and 46.6% of pixels within each plot, with an average shadow cover of 33.9%. Percent shadow cover had a weak, positive correlation with the field-measured green percent canopy area ($R^2 = 0.42$, $P = 0.023$), but was not significantly correlated with field-measured gray or red percent canopy area ($P > 0.05$). The green cover class had the highest percent cover at a majority of the plots, both in the non-normalized and shadow-normalized data. For the green cover class, the mean shadow-normalized cover was 53.3%. The red class had much lower shadow-normalized cover on average (15.2%), although for plot 3 the red shadow-normalized cover reached nearly 50%. Gray shadow-normalized cover averaged 31.5%, but reached as high as 65.7% at plot 2.

Shadow-normalized percent cover aggregated for all plots (53.3% green, 15.2% red, and 31.5% gray) was very similar to the field-measured percent canopy area aggregated for all plots (52.6% green, 16.9% red, and 30.5% gray). Mean absolute error was 8.3% for the green class, 5.4% for the red class, and 7.2% for the gray class. Maximum absolute errors were 16.7% for the green class (plot 11), 12.4% for the red class (plot 4), and 17.5% for the gray class (plot 11). Three-quarters of the GeoEye-1 shadow-normalized cover percentage estimates were within 10% of the field-measured cover percentage estimates. Scatterplots comparing percent cover for the green, red, and gray classes displayed generally linear relationships that closely followed the 1:1 line (Fig. 3). Linear regression equations shown in Fig. 3 have R^2 values ranging from 0.67 to 0.77, slopes close to 1, and y-intercepts within 3.3% of zero. P-values for all regressions were less than 0.001.

As a final analysis step, the classified image was masked for roads, water, and clearings, and the percentage of each shadow-normalized class within the forested area of the Long Lake watershed was calculated. Green was the dominant class, comprising 61.5% of forest area within the watershed. The gray class covered 26.3% of forest area, while the red class comprised the remaining 12.2% of forest area.

4. Discussion

Both the field and remote sensing measures of green, red, and gray canopy cover are imperfect estimates of actual canopy cover within the study area. Due to displacement, registration error, and canopy configuration, trees inside a sample plot can have canopy cover that extends outside of the plot. Conversely, trees outside a sample plot can have canopy cover that extends inside the plot. Displacement of treetops may over-represent the cover of taller trees in the classification. The field sampling did not measure cover within canopy gaps that could also contribute to errors in the classification, although these gaps were largely shadowed in the image. Despite these complications, there was close agreement in the green, red, and gray cover percentages for all twelve of the sample plots, confirming previous studies that have demonstrated the utility of high spatial resolution remotely sensed data for mapping canopy mortality.

This analysis did not address mapping green, red, and gray class cover in non-forested land cover types. To map mountain pine beetle impacts over large areas, clearings, non-forest vegetation, water, and roads would need to be masked or included in the classification training data. The forest surrounding Long Lake is limited to three tree species and dominated by lodgepole pine and subalpine fir. Sites with

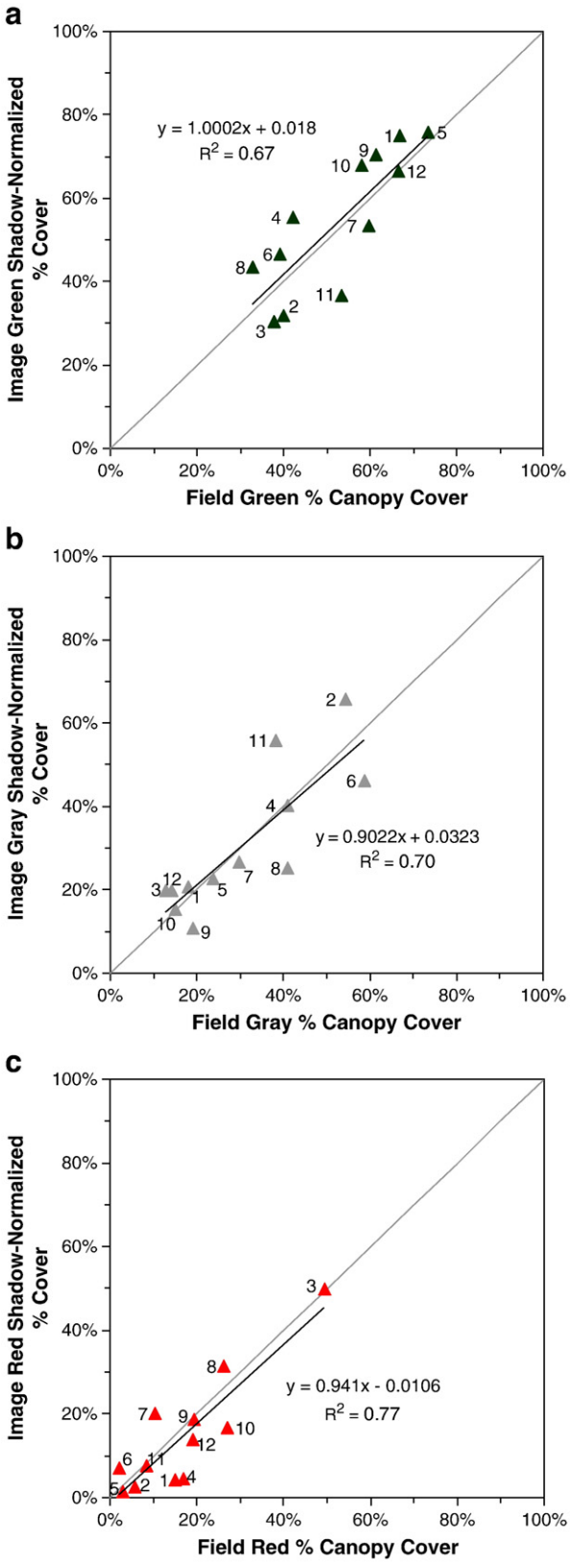

Fig. 3. Field-estimated percent canopy cover vs. shadow-normalized percent cover from the classified GeoEye-1 image. Plots are for green a), red (b), and gray (c) classes. Plot numbers are indicated next to each point.

different mixes of tree species may be more difficult to classify using high spatial resolution satellite data.

While 0.5 m pan-sharpened GeoEye-1 data offer a higher spatial resolution than previously available from spaceborne sensors, certain features of these data may complicate large area monitoring of canopy mortality. The proprietary fusion algorithm used to produce the pan-sharpened product does not preserve radiance, which prevents atmospheric correction and thus prohibits a uniform set of classification rules and makes comparison between multiple images more difficult. Canopy shadowing and displacement are prominent features at 0.5 m resolution, and a potentially wide range of view and solar zenith angles may also make comparison of multiple images more difficult. Finally, the 15.2 km swath width of GeoEye-1 complicates mapping of canopy mortality at regional scales.

In this study, gray canopy cover was distinguishable from green and red canopy cover. However, the gray cover class did not specifically measure lodgepole pine mortality caused by mountain pine beetle. The gray cover class included trees that may have died due to any cause, including subalpine fir and Engelmann spruce. A multitemporal approach capable of capturing the transition from red canopy cover to gray canopy cover is needed to definitively attribute gray canopy cover to attack by mountain pine beetles. However, estimates of gray canopy area may still be useful for understanding ecological disturbance and carbon cycle impacts of disturbance in forest ecosystems.

5. Conclusions

Pan-sharpened, 0.5 m spatial resolution GeoEye-1 data are capable of accurately mapping red and gray canopy cover that are indicators of the severity of an on-going outbreak of mountain pine beetles in a lodgepole pine-dominated forest. While individual tree canopies were not reliably discernable at 0.5 m in our study area, higher spatial resolution data should offer considerable advantages for mapping fine-scale impacts of beetle outbreaks. The utility of non-sharpened and sharpened multispectral data at different spatial resolutions should be compared to determine which data products are most suitable for mapping red and gray canopy cover. As beetle outbreaks continue to decimate conifer forests in western North America, the ability to map both red and gray canopy cover will be increasingly important for monitoring the cumulative impacts of these outbreaks.

Acknowledgements

The authors would like to thank the following people for their valuable contributions to the Long Lake field work: Jessica Spencer, Scott Matheson, Greg Fryer, Doug Bird, and Evan Kraklow.

References

Amman, G. D., & Cole, W. E. (1983). Mountain pine beetle dynamics in lodgepole pine forests. Part II: population dynamics. *USDA Forest Service, Intermountain Forest and Range Experiment Station, General Technical Report INT-145*.

Amman, G. D., & Schmitz, R. F. (1988). Mountain pine beetle-lodgepole pine interactions and strategies for reducing tree losses. *Ambio*, *17*, 62—68.

Breshears, D. D., Cobb, N. S., Rich, P. M., Price, K. P., Allen, C. D., Balice, R. G., et al. (2005). Regional vegetation die-off in response to global-change-type drought. *Proceedings of the National Academy of Sciences USA*, *102*, 15144—15148.

Coops, N. C., Johnson, M., Wulder, M. A., & White, J. C. (2006). Assessment of QuickBird high spatial resolution imagery to detect red attack damage due to mountain pine beetle infestation. *Remote Sensing of Environment*, *103*, 67—80.

Dale, V. H., Joyce, L. A., McNulty, S., Neilson, R. P., Ayres, M. P., Flannigan, M. D., et al. (2001). Climate change and forest disturbances. *BioScience*, *51*, 723—734.

GeoEye. (2009). Website: http://geoeye.com/CorpSite/products/imagery-sources/Default.aspx#geoeye1 Accessed 05 Dec 2009.

Hicke, J. A., & Logan, J. (2009). Mapping whitebark pine mortality caused by a mountain pine beetle outbreak with high spatial resolution satellite imagery. *International Journal of Remote Sensing*, *30*, 4427—4441.

Hill, J. B., Popp, H. W., & Grove, A. R., Jr. (1967). *Botany: A text book for colleges*, fourth ed. Toronto: McGraw-Hill.

Logan, J. A., & Bentz, B. J. (1999). Model analysis of mountain pine beetle (Coleoptera: Scolytidae) seasonality. *Environmental Entomology*, *28*, 924—934.

Logan, J. A., & Powell, J. A. (2001). Ghost forests, global warming, and the mountain pine beetle (Coleoptera: Scolytidae). *American Entomogist*, *47*, 160—172.

Safranyik, L., & Carroll, A. L. (2006). The biology and epidemiology of the mountain pine beetle in lodgepole pine forests. In L. Safranyik, & W. R. Wilson (Eds.), *The mountain pine beetle — a synthesis of biology, management, and impacts in lodgepole pine*. Victoria, British Columbia: Natural Resources Canada, Canadian Forest Service, Pacific Forestry Centre.

Schmid, J. M., & Hinds, T. E. (1974). Development of spruce-fir stands following spruce beetle outbreaks. *USDA Forest Service, Rocky Mountain Forest and Range Experiment Station, Research Paper RM-131, Ogden, UT*.

Schmid, J. M., & Mata, S. A. (1996). Natural variability of specific forest insect populations and their associated effects in Colorado. *USDA Forest Service, Rocky Mountain Forest and Range Experiment Station, General Technical Report RM-GTR-275, Ft. Collins, CO*.

Veblen, T. T., Hadley, K. S., Nel, E. M., Kitzberger, T., Reed, M., & Villalba, R. (1994). Disturbance regime and disturbance interactions in a Rocky Mountain subalpine forest. *Journal of Ecology*, *82*, 125—135.

White, J. C., Wulder, M. A., Brooks, D., Reich, R., & Wheate, R. D. (2005). Detection of red attack stage mountain pine beetle infestation with high spatial resolution satellite imagery. *Remote Sensing of Environment*, *96*, 340—351.

White, J. C., Coops, N. C., Hilker, T., Wulder, M. A., & Carroll, A. L. (2007). Detecting mountain pine beetle red attack damage with EO-1 hyperion moisture indices. *International Journal of Remote Sensing*, *28*, 2111—2121.

Wulder, M. A., White, J. C., Coops, N. C., & Butson, C. R. (2008). Multi-temporal analysis of high spatial resolution imagery for disturbance monitoring. *Remote Sensing of Environment*, *112*, 2729—2740.

Wulder, M. A., Dymond, C. C., White, J. C., Leckie, D. G., & Carroll, A. L. (2006). Surveying mountain pine beetle damage of forests: A review of remote sensing opportunities. *Forest Ecology and Management*, *221*, 27—41.

Wulder, M. A., White, J. C., Bentz, B., Alvarez, M. F., & Coops, N. C. (2006). Estimating the probability of mountain pine beetle red attack damage. *Remote Sensing of Environment*, *101*, 150—166.